THE JOURNAL OF BIOLOGICAL CHEMISTRY VOL. 290, NO. 2, pp. 1096–1105, January 9, 2015

Rheb Protein Binds CAD (Carbamoyl-phosphate Synthetase 2, Aspartate Transcarbamoylase, and Dihydroorotase) Protein in a GTP- and Effector Domain-dependent Manner and Influences Its Cellular Localization and Carbamoyl-phosphate Synthetase (CPSase) Activity*

Received for publication, July 4, 2014, and in revised form, November 21, 2014 Published, JBC Papers in Press, November 24, 2014, DOI 10.1074/jbc.M114.592402

Tatsuhiro Sato[‡1], **Hitomi Akasu**[‡], **Wataru Shimono**[‡], **Chisa Matsu**[‡], **Yuki Fujiwara**[‡], **Yoshio Shibagaki**[‡], **Jeffrey J. Heard**[§], **Fuyuhiko Tamanoi**[§], **and Seisuke Hattori**[‡]

From the [‡]*Division of Biochemistry, School of Pharmaceutical Sciences, Kitasato University, Tokyo 108-8641, Japan and* [§]*Department of Microbiology, Immunology, and Molecular Genetics, Molecular Biology Institute, Jonsson Comprehensive Cancer Center, University of California, Los Angeles, California, 90095*

Background: Rheb activates mTORC1 to stimulate mRNA translation.
Results: Rheb binds to CAD and activates CPSase activity.
Conclusion: Rheb affects intracellular pyrimidine nucleotide pools.
Significance: Our results provide a new mechanism that TSC/Rheb signaling regulates cell growth.

Rheb small GTPases, which consist of Rheb1 and Rheb2 (also known as RhebL1) in mammalian cells, are unique members of the Ras superfamily and play central roles in regulating protein synthesis and cell growth by activating mTOR. To gain further insight into the function of Rheb, we carried out a search for Rheb-binding proteins and found that Rheb binds to CAD protein (carbamoyl-phosphate synthetase 2, aspartate transcarbamoylase, and dihydroorotase), a multifunctional enzyme required for the *de novo* synthesis of pyrimidine nucleotides. CAD binding is more pronounced with Rheb2 than with Rheb1. Rheb binds CAD in a GTP- and effector domain-dependent manner. The region of CAD where Rheb binds is located at the C-terminal region of the carbamoyl-phosphate synthetase domain and not in the dihydroorotase and aspartate transcarbamoylase domains. Rheb stimulated carbamoyl-phosphate synthetase activity of CAD *in vitro*. In addition, an elevated level of intracellular UTP pyrimidine nucleotide was observed in *Tsc2*-deficient cells, which was attenuated by knocking down of Rheb. Immunostaining analysis showed that expression of Rheb leads to increased accumulation of CAD on lysosomes. Both a farnesyltransferase inhibitor that blocks membrane association of Rheb and knockdown of Rheb mislocalized CAD. These results establish CAD as a downstream effector of Rheb and suggest a possible role of Rheb in regulating *de novo* pyrimidine nucleotide synthesis.

Rheb is a member of the Ras superfamily small GTPases that plays important roles in the regulation of protein synthesis and growth in response to nutrient and growth factors (1–5). Small GTPases including Rheb are activated when GTP-bound but inactivated when bound with GDP (6). Although Rheb is conserved from yeast to human, two Rheb proteins termed Rheb1 and Rheb2 have been found only in mouse and human (7). Northern blot analysis has shown that human Rheb1 is ubiquitously expressed, whereas Rheb2 is observed predominantly in the brain and less in the spleen and peripheral blood (8). The two proteins are 52% identical and 73% similar in amino acid sequence. Structurally, the 169 N-terminal residues form a GTPase domain composed of G1-G5 boxes (1, 6, 9). In addition, an isoprenoid farnesyl group is added at a C-terminal CAA*X* (C is cysteine, A is an aliphatic amino acid, and *X* is the C-terminal amino acid) motif (10–12). It has been thought that Rheb1 and Rheb2 have redundant functions (13).

Although Rheb has weak intrinsic GTPase activity, the binding of tuberous sclerosis complex (TSC),[2] TSC1 and TSC2, significantly enhances GTP hydrolysis, leading to the inactivation of Rheb (14–17). Mutations in either the *Tsc1* or *Tsc2* gene results in the hyperactivation of Rheb and causes tuberous sclerosis, an autosomal dominant disease characterized by the development of hamartomas in a variety of organs (18). LKB1- or PTEN-inactivating mutations, which cause inactivation of TSC complex resulting in Rheb activation, also increase the risk of developing cancer. The best-known molecule that mediates Rheb signaling cascades is mTOR, a serine/threonine kinase. This protein forms two distinct complexes, mTORC1 and

* This work was supported, in whole or in part, by National Institutes of Health Grant CA41996 (to F. T.). This work was also supported by Grant-in-aid for Young Scientists B 23790345 (to T. S.) and for Scientific Research C 23510261 (to S. H.).
[1] To whom correspondence should be addressed: Division of Biochemistry, School of Pharmaceutical Sciences, Kitasato University, 5-9-1 Shirokane, Minato-ku, Tokyo 108-8641, Japan. Tel.: 813-5791-6246; Fax: 813-3442-5674; E-mail: satot@pharm.kitasato-u.ac.jp.

[2] The abbreviations used are: TSC, tuberous sclerosis complex; CAD, carbamoyl-phosphate synthetase 2, aspartate transcarbamoylase, and dihydroorotase; CPSase, carbamoyl phosphate synthetase II; PRPP, phosphoribosylpyrophosphate; S6K, S6 kinase; GTPγS, guanosine 5′-*O*-(thiotriphosphate); LAMP2, lysosome-associated membrane protein 2; FTI, farnesyltransferase inhibitor.

mTORC2, and Rheb activates mTORC1. The mTORC1 complex is composed of mTOR, Raptor, and mLST8, whereas mTORC2 contains mTOR, rictor, mLST8, and mSin1 (3). We previously demonstrated that Rheb directly activates mTORC1 and increases the recruitment of its substrate protein eukaryotic initiation factor 4B-binding protein 1 (4E-BP1) (19). The activation of mTORC1 promotes the sequential activation of its substrates such as ribosomal protein S6 kinase 1 (S6K1) and 4E-BP1, leading to cap-dependent mRNA translation initiation.

To gain insight into the function of Rheb, we have undertaken a systematic screen to identify Rheb-binding proteins. Although extensive studies have been carried out on Rheb and mTOR, not much is known about other downstream effectors of Rheb. As multiple effectors have been identified for a variety of small GTPases, it is likely that Rheb activates multiple downstream effectors, but this possibility has not been sufficiently explored. The criteria used to identify Rheb effectors are: (i) the effector binds GTP-bound Rheb but not GDP-bound Rheb, and (ii) the binding requires the presence of an intact effector domain. In this paper we report that one of the proteins, CAD (carbamoyl-phosphate synthetase 2, aspartate transcarbamoylase, and dihydroorotase), a multifunctional enzyme required for the *de novo* synthesis of pyrimidine nucleotides, fulfills these criteria as a potential Rheb effector.

Nucleotide synthesis is a key event for the maximal proliferation of cells because of a limited amount of intracellular nucleotide pools. Thus, the enzymes involved in the nucleotide biosynthetic pathway are attractive targets for growth inhibition of malignant cells. Biosynthesis of nucleotides utilizes ribose 5-phosphate, produced from the oxidative and non-oxidative arms of the pentose phosphate pathway, and nonessential amino acids (20). The rate-limiting step in this pyrimidine synthesis pathway is catalyzed by the carbamoyl phosphate synthetase II (CPSase) of CAD (21, 22). CAD activity is regulated by two molecules. Phosphoribosylpyrophosphate (PRPP), synthesized from ribose 5-phosphate and used for purine and pyrimidine synthesis, increases the CPSase activity of CAD, whereas UTP negatively regulates CPSase activity by feedback inhibition (23). The phosphorylation of CAD by mitogen-activated protein kinase and PKCα changes the CAD sensitivity to UTP and/or PRPP to regulate pyrimidine synthesis. Recently, CAD has been shown to be phosphorylated at serine 1859 by S6K, and this phosphorylation stimulates CAD activity (24, 25). However, the protein that directly regulates CPSase or other enzyme activities in CAD has not been well understood.

In this paper we report that Rheb binds CAD protein. CAD binding to Rheb is specific to the GTP-bound active form of Rheb and is dependent on the presence of an intact effector domain of Rheb. Immunostaining analysis suggests that Rheb recruits CAD to lysosomes, and CAD is mislocalized when the cells are treated with a farnesyltransferase inhibitor, which blocks the membrane binding of Rheb, or transduced with shRNA targeting Rheb. *In vitro* experiments indicated that Rheb stimulated CPSase activity of CAD, although CAD phosphorylation by mTORC1 did not alter the activity. In addition, elevated levels of intracellular pyrimidine nucleotides were observed in *Tsc2*-deficient cells. This increased nucleotide pool persisted even when the cells were treated with rapamycin, whereas knockdown of Rheb reduced UTP pyrimidine nucleotide level. These results suggest that Rheb regulates *de novo* pyrimidine nucleotide synthesis by binding and activating CAD, independent of mTORC1 signaling.

EXPERIMENTAL PROCEDURES

Reagents and Antibodies—Torin1 was a generous gift of Dr. N. Gray (Harvard Medical School). Rapamycin was purchased from Merck Millipore. Insulin was bought from Nacalai Tesque. Antibodies against CAD were purchased from Bethyl Laboratories, anti-Halo antibodies were from Promega, anti-LAMP2 antibody was from Abcam, and anti-AKT, anti-phospho-AKT (Ser-473), anti-S6, anti-phospho-S6 (Ser-235/236), anti-mTOR, and anti-phospho-(Ser) 14-3-3 binding motif antibodies were from Cell Signaling. Anti-FLAG antibody was obtained from Sigma.

Cell Culture and Transfection—The *Tsc2*-deficient mouse renal tumor cell line (E8) and the *Tsc2*-introduced cell line (T2-5) were kindly provided by Dr. O. Hino and Dr. T. Kobayashi. These cells were cultured as previously described (26). HEK293 and HeLa cells were maintained in Dulbecco's modified Eagle's medium (Nissui Seiyaku) supplemented with 10% (v/v) fetal bovine serum and 100 units/ml penicillin and streptomycin. Cells were cultured at 37 °C in a 5% CO_2 incubator. Transfection was carried out using Lipofectamine 2000 (Invitrogen) according to the manufacturer's instructions. For serum starvation, cells were cultured overnight in serum-free medium. Insulin stimulation was performed by incubating serum-starved cells in fresh medium containing 150 nM insulin for 1 h.

DNA Constructs—The plasmid encoding Halo-tagged CAD was purchased from Kazusa DNA Research Institute. Full-length cDNA was digested with BglII and SalI to produce ΔCPS.A (amino acids 931–2162), and the fragment was subcloned into pCMV-Tag 3A vector (Stratagene). Other fragments were amplified by PCR and subcloned into pCMV-Tag 3A vector. pCDNA3-FLAG-Rheb was produced as described previously (27). Y35A, T38A, Q64L, and N153T mutants were generated by site-directed mutagenesis.

Identification of Rheb-binding Proteins—HEK293T cells transfected with the plasmids encoding FLAG-Rheb T38A, Q64L, or GFP (control) and FLAG-Rheb were immunoprecipitated using anti-FLAG M2 affinity gel (Sigma). The cells were lysed with lysis buffer (0.3% CHAPS or 1% Triton X-100, 50 mM Tris-HCl (pH 7.5), 150 mM NaCl, 25 mM $MgCl_2$) containing 1× protease inhibitor mixture (Nacalai Tesque), and the lysates were incubated with anti-FLAG antibody at 4 °C for 3 h.

After washing with lysis buffer, proteins on beads were eluted by the addition of 1× SDS sample buffer (3% SDS, 5% glycerol, 62 mM Tris-HCl (pH 6.8)) and subsequent incubation at 95 °C for 5 min. Protein samples were subjected to SDS-PAGE and stained with SilverQuest silver staining kit (Invitrogen) according to the manufacturer's instructions. Protein bands were then excised from the silver-stained gel, in-gel-digested with trypsin, and subjected to nano-liquid chromatography-electrospray ionization mass spectrometry analysis using a DiNa nano-LC system (KYA Technologies) with an L-column 2 octyldecyl sil-

ane (0.05 mm by 100 mm, 3 μm; CERI) coupled to a QStar Elite hybrid LC-MS/MS system (AB Sciex). Protein identification was performed using Protein Pilot Version 3.0 software (AB Sciex) with default parameters.

Lentivirus-mediated RNAi—shRNA plasmids (pGIPZ shRNAmir) containing the sequence CAGTGTAGTTTGTTGTTTA (shRheb1 #1) or TCAGACATACTCCATAGAT (shRheb1 #2) were used. The plasmids were cotransfected into the HEK293T cells with packaging plasmids using Lipofectamine 2000, and the supernatants containing Rheb1 shRNA viruses were collected after 48 h of incubation. HeLa or E8 cells were infected with lentiviruses in growth medium containing 8 μg/ml Polybrene (Sigma) and selected with 5 μg/ml puromycin (HeLa cells) or 200 μg/ml zeocin (E8 cells) for 2 days.

Intracellular Localization Studies—Cells plated on 15-mm coverslips were immunostained with 5 μM HaloTag TMR Ligand (Promega) for 30 min according to the manufacturer's instructions. Cells were then fixed in PBS containing 1% formaldehyde for 15 min. For lysosome-associated membrane protein 2 (LAMP2) staining, cells were permeabilized in PBS containing 0.1% Triton X-100 for 15 min, incubated with anti-LAMP2 antibody overnight, and stained with fluorescently conjugated secondary antibodies for 1 h. The cells were mounted in Vectashield mounting medium (Vector Laboratories). Fluorescence images were obtained using an Olympus IX71 microscope equipped with a Hamamatsu ORCA-Flash 4.0 CCD monochrome camera (Hamamatsu Photonics).

In Vitro CPSase Assay—Endogenous CAD was immunopurified from HEK293T cells using anti-CAD antibody by the immunoprecipitation method described above. Rabbit IgG was used as a control. The products were mixed in the buffer containing 100 mM Tris-HCl (pH 8.0), 100 mM KCl, 3.3 mM glutamine, 17.5 mM aspartate, 3 mM ATP, 1 mM DTT, 7.5% dimethyl sulfoxide, 10% glycerol, and 5 mM $MgCl_2$. The reaction was initiated by the addition of 1 mM ^{14}C-labeled sodium bicarbonate (40–60 mCi/mmol, PerkinElmer Life Sciences) to a final concentration of 5 mM. The reaction was quenched after 60 min of incubation at 37 °C by the addition of trichloroacetic acid (TCA) to a final concentration of 20%. The samples were heated for 1 h at 95 °C, and then powdered dry ice was added to the tubes to eliminate excess CO_2. Carbon 14-labeled metabolites were counted by a liquid scintillation counter.

Assay for the Nucleotide Pool—Cultured cells (1×10^6) treated with or without rapamycin were lysed with 1 ml of 10% TCA and centrifuged for 2 min at 15,000 rpm. The supernatant was extracted 5–7 times with 500 μl of diethyl ether until the pH was >5.0. The extract was reduced to a volume of <200 μl by a SpeedVac concentrator (TOMY SEIKO) and analyzed by high performance liquid chromatography (HPLC). The sample was injected onto a column (100 × 4.6 mm) of Partisil-10 SAX anion-exchange resin (Reeve Angel) equilibrated with Buffer A (7 mM ammonium phosphate buffer at pH 3.8). The nucleotides were eluted with a discontinuous gradient of Buffer A and Buffer B (250 mM ammonium phosphate buffer, 500 mM KCl (pH 4.5)) at a flow rate of 1 ml/min. Buffer B increased linearly to 40% in 5 min, from 40% to 60% in 20 min and then to 100% over the next 5 min. The absorbance at 254 and 280 nm was monitored continuously. The peaks were analyzed using the ChromNAV software (Jasco). The identification and amount of each nucleotide were calculated from standard curves obtained using authentic standards.

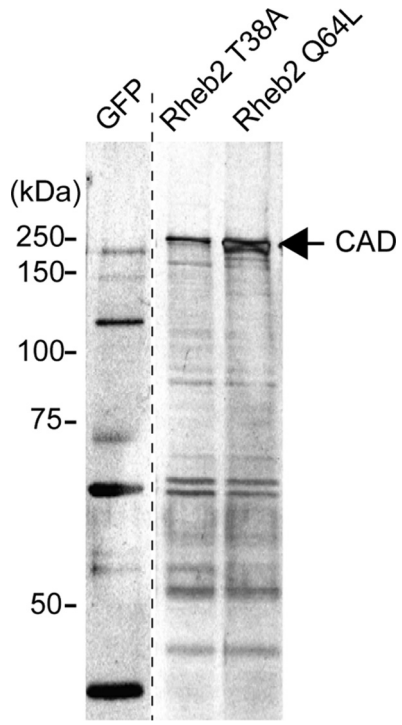

FIGURE 1. **Identification of CAD as a Rheb2-binding protein.** HEK293T cells were transfected with the vector encoding GFP (control), Rheb2 T38A negative mutant, or Q64L active mutant. The cell lysates were immunoprecipitated with anti-FLAG antibody, and the products were resolved by SDS-PAGE followed by silver staining. Molecular weight markers in kilodaltons are shown on the *left side of the gel*. CAD was identified by LC-MS/MS.

RESULTS

Identification of CAD as a Rheb2-binding Protein—To identify new Rheb effectors, we decided to screen for a protein whose binding depends on the presence of an intact effector domain. Initially, we tested both Rheb1 and Rheb2, but Rheb2 gave more pronounced results. We previously showed that a mutation of residue Thr-38 within the effector domain of Rheb1 results in the inability of Rheb1 to activate mTORC1 while maintaining a normal level of GTP binding (19). Thus, a mutant form of Rheb2, Rheb2 (T38A) and an active mutant of Rheb2, Rheb2^{Q64L}, was used. These mutants as well as a GFP control were expressed as FLAG-tagged proteins in HEK293T cells. Cell lysates were immunoprecipitated with anti-FLAG antibody, and Rheb-interacting proteins were visualized by SDS-PAGE and protein silver staining. An intense band of ~250-kDa was observed in the sample with Rheb2^{Q64L}, whereas the band was significantly weak or not detected in Rheb2^{T38A} and in the control sample (Fig. 1). We thus analyzed the protein sequence in the band using liquid chromatography coupled with tandem mass spectrometry (LC-MS/MS) systems and identified CAD as a Rheb2-binding protein (ProteinPilot score: 99.86).

Both Rheb1 and Rheb2 Bind CAD, but Rheb2 Binds Better with CAD—To confirm the interaction between Rheb and CAD, we co-expressed FLAG-Rheb1 or FLAG-Rheb2 with

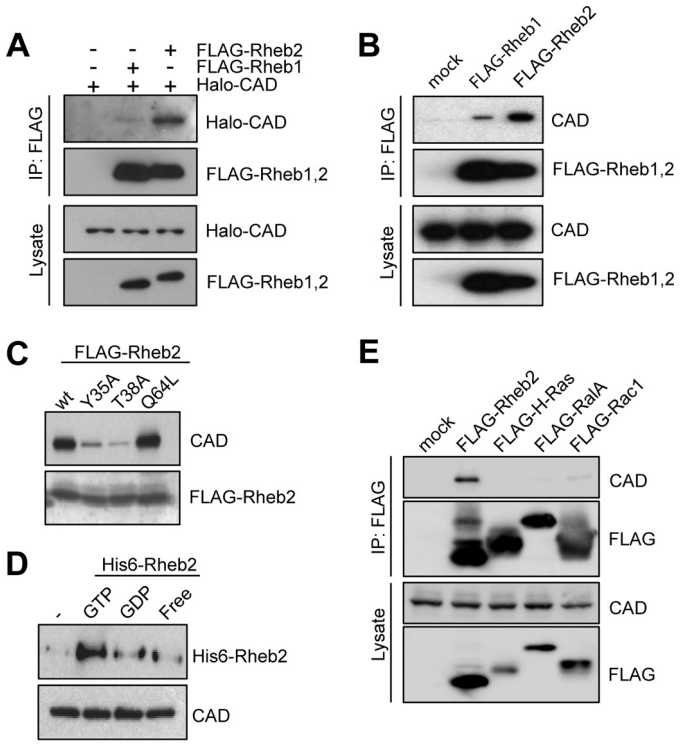

FIGURE 2. **Specific binding of Rheb to CAD.** *A–C*, HEK293T cells expressing the indicated proteins were subjected to immunoprecipitation (*IP*) with anti-FLAG antibody. Co-precipitation of Halo-CAD (*A*) or endogenous CAD (*B* and *C*) was detected by Western blotting. *D*, His6-fusion Rheb2 loaded with GTPγS, GDP, or EDTA only (nucleotide free) was incubated with HEK293T cell lysates and subjected to immunoprecipitation with anti-CAD antibody. The precipitates were analyzed by Western blotting. *E*, HEK293T cells expressing FLAG-tagged active mutant of small GTPase (Rheb2 Q64L, H-Ras G12V, RalA G23V, or Rac1 G12V) were subjected to immunoprecipitation with anti-FLAG antibody. Co-precipitation of endogenous CAD was detected by Western blotting.

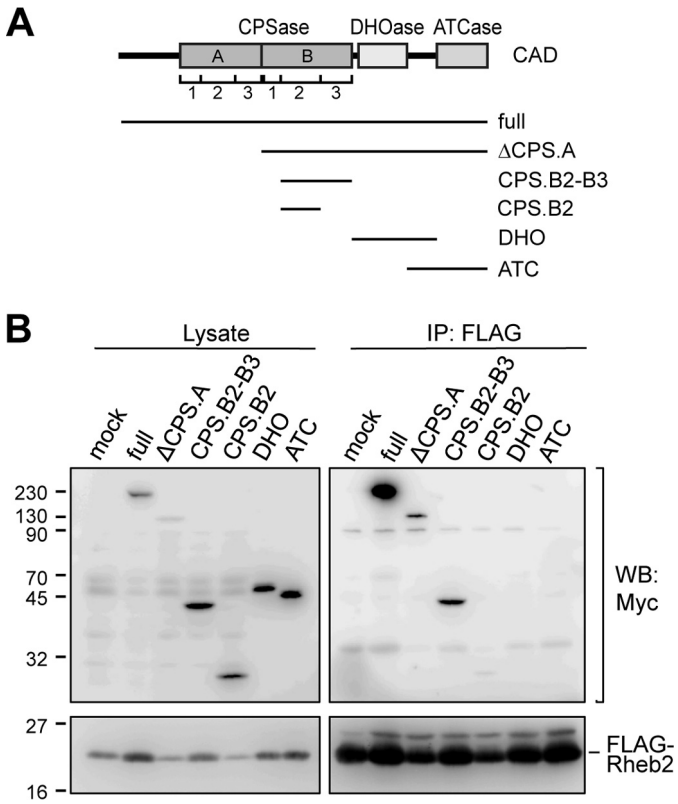

FIGURE 3. **Defining the region of CAD where the Rheb interaction takes place.** *A*, domain arrangement of CAD. An N-terminal CPSase domain is followed by a regulatory region (B3), a dihydroorotase, and a C-terminal aspartate transcarbamoylase (*ATC*). The indicated CAD fragments were used in *B*. *B*, HEK293T cells expressing indicated the Myc-CAD fragment and FLAG-Rheb2 Q64L were subjected to immunoprecipitation (*IP*) with anti-FLAG antibody. Co-precipitation of FLAG-Rheb2 and Myc-tagged CAD fragments was detected by Western blotting (*WB*).

Halo-CAD and co-precipitation assays were performed in Fig. 2*A*. Both Rheb1, and Rheb2 were shown to co-immunoprecipitate with CAD. The amount of CAD precipitated with Rheb2 was much higher than that with Rheb1, suggesting a stronger interaction of CAD with Rheb2. Fig. 2*B* shows co-immunoprecipitation of endogenous CAD with Rheb1 or Rheb2. This was shown by expressing FLAG-Rheb1 or FLAG-Rheb2 alone and probing the immunoprecipitate with anti-CAD antibody. These results confirm binding of Rheb with CAD. As Rheb2 exhibits more pronounced binding with CAD compared with Rheb1, we used Rheb2 in the following experiments.

Specific Interaction of CAD with the GTP Form of Rheb—Although we identified CAD by using the Rheb2^{Q64L} mutant in our initial screen, we observed significant amounts of CAD binding to the wild type Rheb2 (Fig. 2*C*). This is because the wild type Rheb overexpressed in mammalian cells exists as an active form because of weak intrinsic GTPase activity and a limiting amount of TSC1/2 (28). In contrast, little binding of CAD was observed with two different effector domain mutants of Rheb2, alanine substitution mutant at residue 35 that reduces the amount of nucleotide bound to Rheb as well as the mutant at residue 38 that decreases effector activation without significantly affecting GTP binding activity (19). Taken together, it appears that CAD selectively binds to an active form of Rheb.

To further examine GTP dependence of CAD binding, recombinant Rheb loaded with GTPγS, GDP, or a nucleotide-free form of Rheb was added to lysates of HEK293T cells, and endogenous CAD was immunoprecipitated with anti-CAD antibody (Fig. 2*D*). The band of Rheb-GTP was clearly detected. On the other hand, Rheb-GDP and the nucleotide-free form of Rheb were hardly detected in the CAD precipitate.

Finally, we examined whether other members of the Ras superfamily G-proteins bind CAD. In this experiment various small GTPases were expressed in HEK293T cells, and co-immunoprecipitation of CAD was examined. As shown in Fig. 2*E*, CAD was co-precipitated with Rheb^{Q64L} but not with the active small GTPase mutants such as H-Ras^{G12V}, RalA^{G17V}, and Rac1^{Q61L}, indicating that CAD specifically interacts with active form of Rheb.

Rheb Binds to the CPSase Regulatory Region of CAD—Deletion constructs of CAD were used to delineate the region of CAD where Rheb interacts. Myc-CAD deletion constructs shown in Fig. 3*A* were generated and used to co-transfect with FLAG-Rheb2 construct into HEK293T cells. Rheb2 was immunoprecipitated by using anti-FLAG antibody, and the presence of CAD was examined. As shown in Fig. 3*B*, full-length, ΔCPS.A, CPS.B2-B3 fragment, and to a much lesser extent CPS.B2 interacted with Rheb. On the other hand, fragments containing only the dihydroorotase domain or aspartate tran-

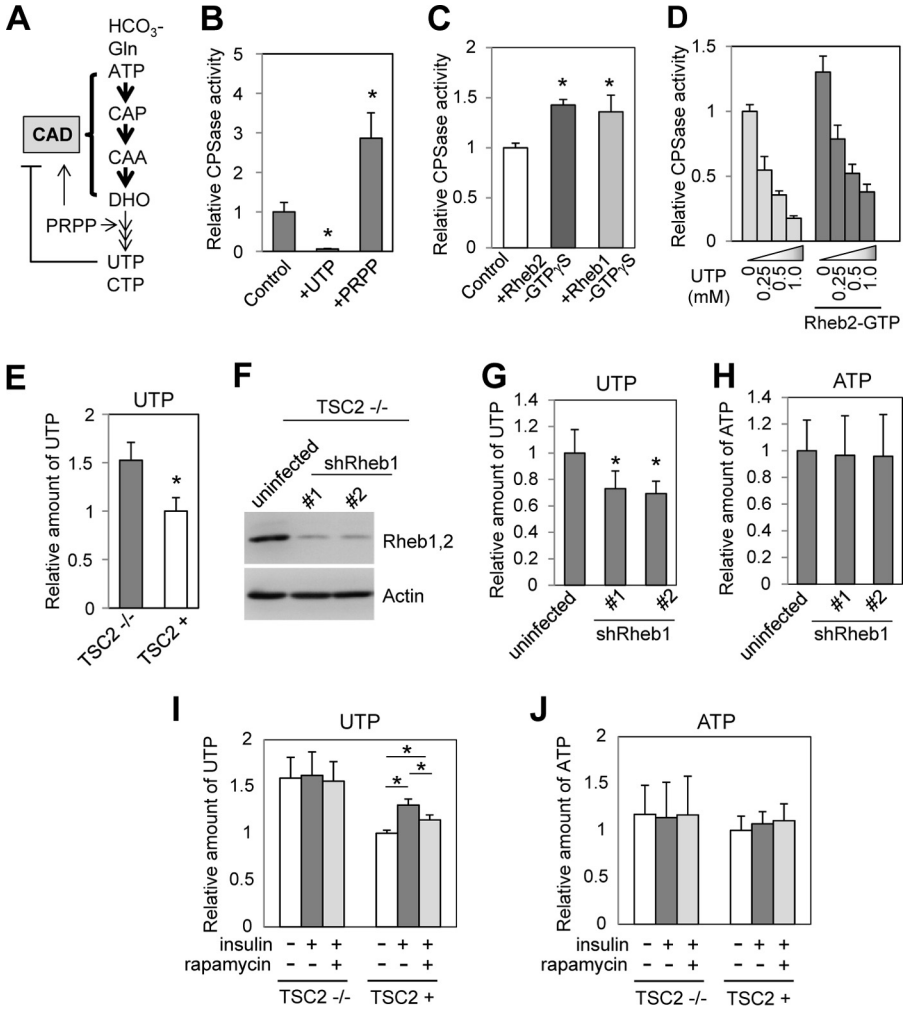

FIGURE 4. **Rheb activates CAD and alters intracellular nucleotide pools.** *A*, role of CAD in pyrimidine biosynthesis. CAD exerts the first three steps, in which first CPSase reaction catalyzes a rate-limiting step. CAD activity is negatively regulated by UTP, a final product of this pathway, but activated by PRPP, a biosynthetic precursor of pyrimidine and purine nucleotides. *CAA*, carbamoyl acetic acid; *DHO*, dihydroorotate. *B–D*, after immunoprecipitation of endogenous CAD, *in vitro* CPSase assays were performed in the absence (*Control*) or presence of UTP, PRPP, Rheb2-GTPγS, or Rheb1-GTPγS. *Bars* represent the relative CPSase activities in three independent experiments with S.D. *E*, *Tsc2*-deficient renal tumor (E8) cells and *Tsc2*-replete (T2-5) cells were lysed, and the intracellular UTP was separated by HPLC. *Bars* show relative amounts of UTP in three independent experiments with S.D. *F–H*, E8 cells infected with lentiviruses expressing shRNA against Rheb1 (*shRheb1 #1* or *#2*) were lysed, and the proteins were subjected to Western blotting (*F*). The intracellular UTP and ATP were separated by HPLC (*G* and *H*). *Bars* represent the relative amount of indicated nucleotides in three different experiments with S.D. *, $p < 0.05$ *versus* control. *I* and *J*, after E8 and T2-5 cells were treated with DMSO, 150 nM insulin, or the combination of insulin and 100 nM rapamycin for 2 h, these cells were lysed, and the intracellular UTP and ATP were separated by HPLC. *Bars* represent the relative amount of indicated nucleotide in three different experiments with S.D. *, $p < 0.05$ *versus* control.

scarbamoylase domain did not bind Rheb. These results place the interaction domain in the region B of the CPSase domain. Interestingly, this region overlaps with the regulatory region of CAD where UTP and PRPP bind and cause allosteric regulation of CPSase (29).

Rheb Stimulates CPSase Activity of CAD—The specific binding of Rheb-GTP to CAD led us to examine whether Rheb regulates CAD activity. CAD has three enzyme activities and catalyzes the first three steps in *de novo* pyrimidine nucleotide biosynthesis (21, 22) (Fig. 4*A*). CPSase of CAD is responsible for the catalysis of the first rate-limiting step of *de novo* pyrimidine biosynthesis. This activity is allosterically inhibited by the UTP, an end product, and activated by PRPP, a substrate for pyrimidine and purine biosynthesis (23). To assess the effect of Rheb on CPSase activity, we first checked whether immunopurified CAD can be used for an *in vitro* CPSase assay.

Endogenous CAD was immunoprecipitated from HEK293T cell lysate using anti-CAD antibody and incubated with ^{14}C-labeled sodium bicarbonate, glutamine, and aspartate in the presence or absence of UTP or PRPP for 60 min at 37 °C. As shown in Fig. 4*B*, UTP inhibited CPSase activity, whereas PRPP activated CPSase activity, suggesting that the regulation of CPSase can be evaluated by this method. We next measured the CPSase activity in the presence of Rheb (Fig. 4*C*). The CPSase activity was significantly increased by the addition of Rheb2-GTPγS. Rheb1-GTPγS also stimulated the CPSase activity to a similar extent.

Previous results have shown that the modification of Ser-1406 in the regulatory subdomain abolishes UTP- and PRPP-dependent regulation of CPSase (30). Thus, we tested whether Rheb counteracts the inhibitory effect of UTP on CPSase (Fig. 4*D*). However, UTP inhibited CPSase activity even in the pres-

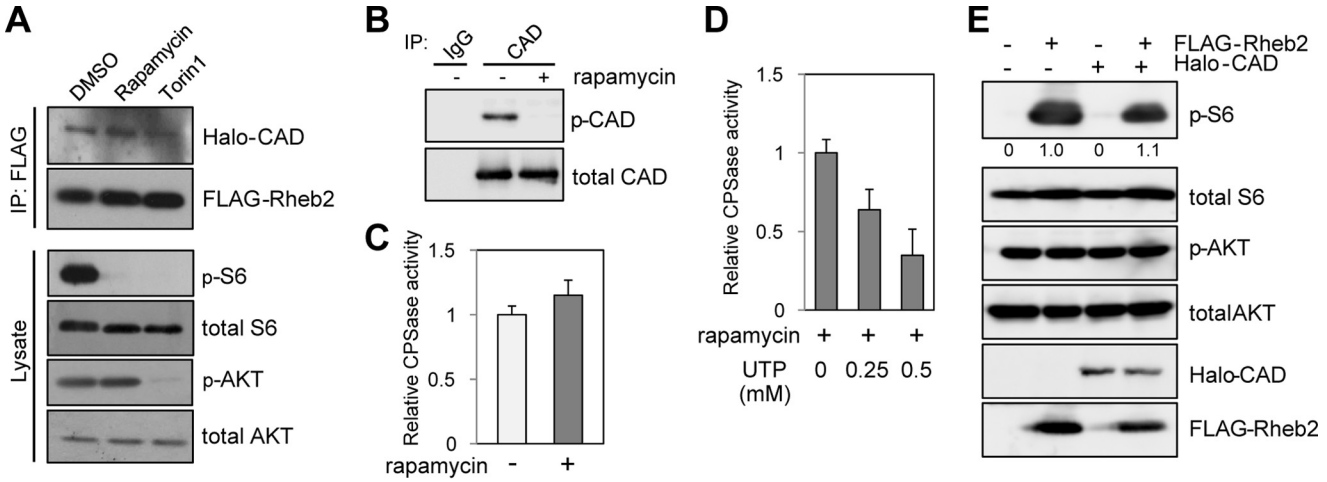

FIGURE 5. **mTORC1 inhibition does not influence Rheb-CAD interaction.** *A*, after the treatment with DMSO, 100 nM rapamycin, or 100 nM Torin1 for 1 h, HEK293T cells expressing FLAG-Rheb2 and Halo-CAD were subjected to immunoprecipitation (*IP*) with anti-FLAG antibody. *WCL*, whole cell lysates. *B* and *C*, HEK293T cells treated with DMSO or rapamycin were subjected to immunoprecipitation with anti-CAD antibody. Aliquots were subjected to Western blotting (*B*) and the *in vitro* CPSase assay (*C*). The phosphorylation of CAD was detected using anti-phospho-Ser 14-3-3 binding motif antibody. *Bars* represent the relative CPSase activities in three independent experiments with S.D. *D*, HEK293T cells treated with rapamycin were subjected to immunoprecipitation with anti-CAD antibody, and then the products were used for *in vitro* CPSase assay in the presence or absence of UTP. *Bars* represent the relative CPSase activities in three independent experiments with S.D. *E*, HEK293T cells expressing the indicated proteins were lysed, and the phosphorylation of S6 and AKT were analyzed by Western blotting. The relative intensity of phospho-S6 was normalized to total S6 (control, Halo-CAD) or total S6 and FLAG-Rheb2 (FLAG-Rheb2, FLAG-Rheb2+Halo-CAD).

ence of Rheb2 in a dose-dependent manner, suggesting that Rheb2 activates CAD but does not abrogate the negative feedback regulation by UTP.

Tsc-deficient Cells Exhibit Increased Levels of Intracellular Pyrimidine Pools—In *Tsc*-deficient cells, the amount of GTP-bound Rheb is increased due to the absence of the GAP activity of TSC, resulting in Rheb activation (14). To examine whether this increased Rheb activity is associated with an increase in pyrimidine biosynthesis, we examined the pool of UTP by using HPLC in *Tsc*-deficient cells. We used *Tsc2*-deficient mouse renal tumor cell line (E8) and its control T2-5 that has *Tsc2* reintroduced. As shown in Fig. 4*E*, the level of UTP in the E8 *Tsc2*-deficient renal tumor cells was significantly higher than that in the control T2-5 cells.

To further examine whether the high level of pyrimidine nucleotide in *Tsc*-deficient cells is controlled by Rheb, Rheb was knocked down by RNA interference. Knockdown of total Rheb in E8 cells was confirmed by Western blotting using the antibody recognizing both Rheb1 and Rheb2 (Fig. 4*F*). The UTP level was reduced by 26% (shRheb1 #1) to 31% (shRheb1 #2) by the knockdown of Rheb, whereas the ATP level was not significantly altered (Fig. 4, *G* and *H*). These results indicate that Rheb plays important roles in pyrimidine synthesis in *Tsc2*-deficient renal tumor cells.

The low level of UTP pool in the control T2-5 cells was increased to a level comparable with that in the E8 cells when the cells were stimulated by the addition of insulin. This increase was partially inhibited by the treatment with rapamycin (Fig. 4*I*). On the other hand, the level of UTP in the E8 cells was up-regulated, and this increased level was unaffected by insulin as well as by rapamycin. The result with rapamycin is consistent with the idea that the increased UTP is mainly due to Rheb activation than to mTOR/S6K activation. We also examined a purine nucleotide pool of ATP (Fig. 4*J*). This ATP pool was similar between E8 and T2-5 cells and was not influenced by insulin or rapamycin.

mTORC1-dependent Phosphorylation of CAD Does Not Affect the Interaction of Rheb and CAD—Recent studies have shown that mTORC1 activation of S6K phosphorylates CAD at Ser-1859, leading to the stimulation of *de novo* pyrimidine biosynthesis (24, 25). This raises the question of possible interplay between Rheb, mTOR, and CAD. For example, mTORC1-dependent phosphorylation of CAD may enhance the interaction with Rheb, resulting in the activation of CAD. This possibility was evaluated by expressing FLAG-Rheb in HEK293T cells, treating with rapamycin, an mTORC1 inhibitor, or Torin1, an mTOR kinase inhibitor, and the interaction of Rheb with CAD was examined by immunoprecipitation assay (Fig. 5*A*). The specific inhibition of mTORC1 by rapamycin was confirmed by the down-regulation of phospho-S6, whereas the inhibition of mTORC1 and mTORC2 by Torin1 was confirmed by decreasing the phosphorylation level of both S6 and AKT. As reported (24, 25), rapamycin treatment inhibited phosphorylation of CAD, whereas the CPSase activity was not affected and remained sensitive to UTP inhibition (Fig. 5, *B–D*). The results on Rheb-CAD interaction showed that the amount of CAD bound to Rheb was not affected by rapamycin (Fig. 5*A*).

We also asked whether CAD has effects on mTORC activities. To examine this point, Rheb2 and/or CAD were expressed in HEK293T cells, and effects on mTORC1 or mTORC2 were examined by the phosphorylation of S6 or AKT (Fig. 5*E*). As can be seen, CAD expression did not affect phosphorylation of S6 or AKT. Furthermore, co-expression of CAD with Rheb2 did not increase phosphorylation of S6 induced by Rheb expression. These results suggest that CAD does not affect mTORC1 or mTORC2 activities.

Rheb Affects Cellular Localization of CAD—As Rheb is required for mTORC1 activation but not for the recruitment of

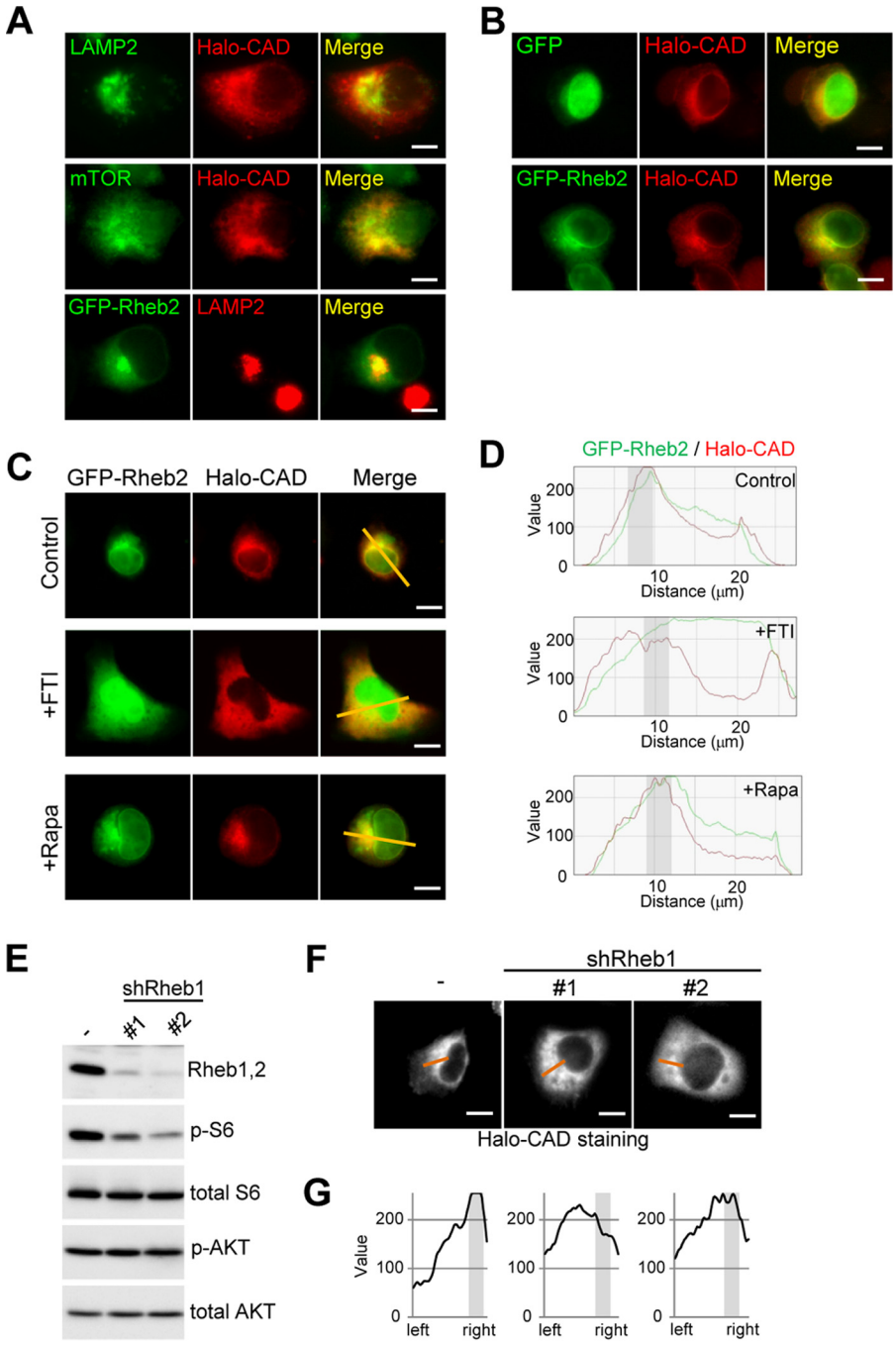

FIGURE 6. **Colocalization of Rheb and CAD at lysosomal membranes.** *A*, Halo-CAD or GFP-Rheb2 was expressed in HeLa cells. Halo was labeled with HaloTag TMR ligand 30 min before fixation. LAMP2 and mTOR were stained with specific antibodies, respectively, after fixation. *B*, the cells expressing GFP and Halo-CAD or GFP-Rheb2 and Halo-CAD were stained with HaloTag TMR ligand 30 min before fixation. *C*, the cells expressing GFP-Rheb2 and Halo-CAD were treated with 10 μM FTI-277 (*FTI*) or 100 nM rapamycin (*Rapa*) for 24 or 1 h, respectively. Halo was labeled with HaloTag TMR ligand 30 min before fixation. *D*, graphs show line plot quantifications of GFP-Rheb and Halo-CAD fluorescent intensity depicted in *C*. *E*, HeLa cells (−) and the cells infected with lentiviruses expressing shRNA against Rheb1 (*shRheb1 #1* and *#2*) were lysed, and the proteins were subjected to Western blotting. *F*, after the cells shown in *E* were transfected with the plasmid encoding Halo-CAD, Halo was labeled with HaloTag TMR ligand 30 min before fixation. *G*, graphs show line plot quantifications of Halo-CAD fluorescent intensity depicted in *F*.

mTORC1 to proper cellular location (31), we examined whether Rheb affects cellular localization of CAD in cultured cells. We first examined the localization of Halo-CAD expressed in HeLa cells. The signal was observed in the cytosol surrounding the nucleus (perinuclear) and partially co-localized with LAMP2, a lysosomal marker, and mTOR (Fig. 6*A*, *top* and *middle panels*). This CAD localization appears to be different from that of Rheb, as the localization of GFP-Rheb2 was more restricted, showing signal only at one side of perinuclear region and mostly colocalized with LAMP2 (Fig. 6*A*, *bottom panels*).

However, when GFP-Rheb and Halo-CAD were co-expressed, the localization of CAD and Rheb became quite similar. CAD staining was mainly concentrated in a restricted peri-

nuclear region, and this localization overlapped with that of GFP-Rheb2 (Fig. 6*B*). On the other hand, CAD was observed in the perinuclear region when co-expressed with GFP as a control. These results suggest that the expression of GFP-Rheb2 results in the accumulation of CAD on lysosomes. These results are significant, as the Rheb/mTORC1 signaling is mainly regulated on the lysosomal membranes (3).

To further examine whether Rheb affects CAD localization on lysosomal membranes, cells were treated with a farnesyltransferase inhibitor (FTI), which interferes with membrane association of Rheb by inhibiting the farnesylation of Rheb at the C-terminal CAA*X* box. In the cells treated with FTI, localization of both Rheb and CAD was drastically changed; GFP-Rheb was detected mainly in nucleus as observed for GFP in Fig. 6*C*, whereas CAD was distributed throughout the cytoplasm (Fig. 6*C*). As seen in Fig. 6*D*, specific accumulation of Rheb and CAD signals at the perinuclear region (shown as shading) in the control cells were widely dispersed by FTI treatment, suggesting that the mislocalization of ectopically expressed GFP-Rheb as well as endogenously expressed Rheb completely abolished the accumulation of CAD to lysosomes. In contrast, the inactivation of mTORC1 by rapamycin did not significantly alter CAD localization, and CAD accumulated at the perinuclear region with Rheb (Fig. 6, *C* and *D*, *lower panels*).

To further analyze whether Rheb recruits CAD, we examined shRNA-mediated Rheb knockdown in HeLa cells. Western blotting analysis using the antibody recognizing both Rheb1 and Rheb2 showed the suppression of Rheb and its downstream signal assessed by phospho-S6 in the knockdown cells (Fig. 6*E*). Halo-CAD diffused freely in the cytoplasm by the knockdown of Rheb, whereas CAD showed the restricted distribution in the control cells (Fig. 6, *F* and *G*). These results indicate that Rheb affects cellular localization of CAD.

DISCUSSION

This paper represents our first report of proteins binding to Rheb. We have undertaken a systematic screen to identify Rheb-binding proteins. As can be seen in Fig. 1, multiple proteins were co-purified with Rheb2. Our strategy was to take advantage of Rheb effector domain mutants we generated before (19). In particular, the T38A mutant exhibits normal levels of GTP binding but cannot activate downstream effectors. One of the prominent bands was found to represent CAD, a multifunctional enzyme involved in pyrimidine biosynthesis. We also showed that another effector domain mutant of Rheb, Y35A, is defective in the binding to CAD. Indeed, further characterizations established that Rheb binding to CAD is specific, as we did not detect binding of other Ras superfamily GTPases (H-Ras, RalA, Rac1) to CAD. Furthermore, we demonstrated that the binding of Rheb to CAD is GTP-dependent, as GDP-bound or nucleotide-free Rheb did not bind CAD. Although a number of attempts have been made to identify Rheb-binding proteins, no clear candidates have emerged before. One of the reasons for the successes of our screen is the use of Rheb2; Rheb2 has a stronger binding to binding proteins. Although Rheb1 also binds CAD, the binding is weaker compared with that of Rheb2 (Fig. 2).

We have defined the region of CAD where Rheb interacts. CAD is a multifunctional enzyme with three different activities, CPSase, dihydroorotase, and aspartate transcarbamoylase. Each activity is coded in a separate domain. Our deletion analysis points to region B of the CPSase. Thus, Rheb does not bind to the dihydroorotase and aspartate transcarbamoylase domains. In support of this idea, our *in vitro* assays demonstrated that Rheb can activate CPSase activity of CAD. Our analysis revealed that a B2-B3 fragment of CAD efficiently binds Rheb. Interestingly, this region overlaps with the regulatory region of CPSase whose activity is regulated by UTP and PRPP (23). This raised the possibility that Rheb is competing with these regulators; however, Rheb-activated CPSase activity was still sensitive to the inhibition by UTP, suggesting that Rheb did not influence UTP inhibition. Further studies are needed to examine whether Rheb affects allosteric regulation of CAD.

It is important to point out that the Rheb binding region we identified is located away from serine 1859 where phosphorylation by S6K takes place (24, 25). This mTOR-dependent phosphorylation occurs at a site located between the dihydroorotase and aspartate transcarbamoylase domains. Although Rheb is an activator of mTORC1, it appears that the CAD phosphorylation and Rheb binding are two separate events. First, the inhibitors of mTORC1 did not affect binding of Rheb to CAD. Second, rapamycin treatment did not significantly affect CPSase activity of CAD. In addition, expression of Rheb2 and CAD did not affect the activity of mTORC1 as examined by the phosphorylation of S6. Taken together, these results suggest that CAD can be activated by two different mechanisms, phosphorylation at Ser-1859 and Rheb binding. Because phosphorylation was shown to induce CAD oligomerization (24), these two events have different outcomes.

Significance of Rheb in pyrimidine biosynthesis is gleaned from our characterization of *Tsc2*-deficient cells (Fig. 4). In our study with a pair of mouse renal tumor cell lines, we found that the pool of UTP, but not ATP, is increased in *Tsc2*-deficient cells and that the knockdown of Rheb significantly reduced the UTP levels. Rheb may be strongly activated in *Tsc2*-deficient cells, resulting in nearly full activation of CAD in the pyrimidine synthesis pathway, which was not stimulated further by insulin. Rapamycin inhibition of mTORC1 little affected the UTP levels in these cells, possibly because mTORC1-dependent stimulation of CAD may be marginal. In contrast, it appears that both mTORC1-dependent and -independent (likely Rheb-dependent) regulation of pyrimidine synthesis occur in T2-5 ($Tsc2^{+}$) cells stimulated with insulin; thus, rapamycin only inhibited the mTORC1-dependent portion.

One of the interesting findings we made concerns cellular localization of CAD. Indirect immunofluorescence of CAD shows localization of this metabolic enzyme widely in the cytoplasm and perinuclear region. However, CAD localization becomes concentrated in the perinuclear region when Rheb is co-expressed. The CAD stain overlaps with that of LAMP2, suggesting that CAD is localized on lysosomes in the presence of excess Rheb. The perinuclear, punctuate staining of Rheb2 is consistent with earlier observations suggesting the presence of Rheb on endosomes and lysosomes (8, 32). We observe over-

lapping localization of Rheb2 and CAD. These results suggest that Rheb recruits CAD to a vesicular localization where Rheb catalyzes multiple functions. Interestingly, FTI treatment dramatically changed cellular localization of both Rheb2 and CAD. Because Rheb2 ends with the CAA*X* motif and it is farnesylated, the FTI treatment inhibits its farnesylation, leading to cytosolic localization of Rheb. FTI treatment or knockdown of Rheb causes CAD to return to a generally cytoplasmic localization. These results point to the function of Rheb to place CAD at a particular cellular location needed to support its function. Pyrimidine biosynthesis uses glutamine as a starting material to synthesize UTP. Recent studies suggest that amino acids are taken up into cells and accumulate on lysosomes (33). Thus, CAD localization to lysosomes may be a mechanism to place this multifunctional enzyme close to glutamine, the amino acid source needed for pyrimidine biosynthesis.

As shown in Fig. 1, multiple protein bands were identified by the Rheb2 pulldown. Thus, there are proteins other than CAD that bind Rheb. Characterization of these proteins is ongoing, and this should result in dramatically expanding our knowledge on the Rheb GTPases.

Acknowledgments—We thank Dr. O. Hino and Dr. T. Kobayashi for providing E8 and T2-5 cell lines, Dr. N. Gray for providing Torin1, and J. Tsukada for technical assistance. We thank Dr. Kenneth A. Bradley and Dr. Robert Damoiseaux at UCLA MSSR (Molecular Screening Shared Resource) for providing shRNA materials and guidance.

REFERENCES

1. Aspuria, P. J., and Tamanoi, F. (2004) The Rheb family of GTP-binding proteins. *Cell. Signal.* **16,** 1105–1112
2. Jewell, J. L., Russell, R. C., and Guan, K. L. (2013) Amino acid signalling upstream of mTOR. *Nat. Rev. Mol. Cell Biol.* **14,** 133–139
3. Laplante, M., and Sabatini, D. M. (2012) mTOR signaling in growth control and disease. *Cell* **149,** 274–293
4. Avruch, J., Hara, K., Lin, Y., Liu, M., Long, X., Ortiz-Vega, S., and Yonezawa, K. (2006) Insulin and amino-acid regulation of mTOR signaling and kinase activity through the Rheb GTPase. *Oncogene* **25,** 6361–6372
5. Heard, J. J., Fong, V., Bathaie, S. Z., and Tamanoi, F. (2014) Recent progress in the study of the Rheb family GTPases. *Cell. Signal.* **26,** 1950–1957
6. Vetter, I. R., and Wittinghofer, A. (2001) The guanine nucleotide-binding switch in three dimensions. *Science* **294,** 1299–1304
7. Patel, P. H., Thapar, N., Guo, L., Martinez, M., Maris, J., Gau, C. L., Lengyel, J. A., and Tamanoi, F. (2003) Drosophila Rheb GTPase is required for cell cycle progression and cell growth. *J. Cell Sci.* **116,** 3601–3610
8. Saito, K., Araki, Y., Kontani, K., Nishina, H., and Katada, T. (2005) Novel role of the small GTPase Rheb: its implication in endocytic pathway independent of the activation of mammalian target of rapamycin. *J. Biochem.* **137,** 423–430
9. Bourne, H. R., Sanders, D. A., and McCormick, F. (1991) The GTPase superfamily: conserved structure and molecular mechanism. *Nature* **349,** 117–127
10. Clark, G. J., Kinch, M. S., Rogers-Graham, K., Sebti, S. M., Hamilton, A. D., and Der, C. J. (1997) The Ras-related protein Rheb is farnesylated and antagonizes Ras signaling and transformation. *J. Biol. Chem.* **272,** 10608–10615
11. Urano, J., Tabancay, A. P., Yang, W., and Tamanoi, F. (2000) The Saccharomyces cerevisiae Rheb G-protein is involved in regulating canavanine resistance and arginine uptake. *J. Biol. Chem.* **275,** 11198–11206
12. Yang, W., Tabancay, A. P., Jr., Urano, J., and Tamanoi, F. (2001) Failure to farnesylate Rheb protein contributes to the enrichment of G_0/G_1 phase cells in the *Schizosaccharomyces pombe* farnesyltransferase mutant. *Mol. Microbiol.* **41,** 1339–1347
13. Tabancay, A. P., Jr., Gau, C. L., Machado, I. M., Uhlmann, E. J., Gutmann, D. H., Guo, L., and Tamanoi, F. (2003) Identification of dominant negative mutants of Rheb GTPase and their use to implicate the involvement of human Rheb in the activation of p70S6K. *J. Biol. Chem.* **278,** 39921–39930
14. Garami, A., Zwartkruis, F. J., Nobukuni, T., Joaquin, M., Roccio, M., Stocker, H., Kozma, S. C., Hafen, E., Bos, J. L., and Thomas, G. (2003) Insulin activation of Rheb, a mediator of mTOR/S6K/4E-BP signaling, is inhibited by TSC1 and 2. *Mol. Cell* **11,** 1457–1466
15. Tee, A. R., Manning, B. D., Roux, P. P., Cantley, L. C., and Blenis, J. (2003) Tuberous sclerosis complex gene products, Tuberin and Hamartin, control mTOR signaling by acting as a GTPase-activating protein complex toward Rheb. *Curr. Biol.* **13,** 1259–1268
16. Inoki, K., Li, Y., Xu, T., and Guan, K. L. (2003) Rheb GTPase is a direct target of TSC2 GAP activity and regulates mTOR signaling. *Genes Dev.* **17,** 1829–1834
17. Zhang, Y., Gao, X., Saucedo, L. J., Ru, B., Edgar, B. A., and Pan, D. (2003) Rheb is a direct target of the tuberous sclerosis tumour suppressor proteins. *Nat. Cell Biol.* **5,** 578–581
18. van Eeghen, A. M., Black, M. E., Pulsifer, M. B., Kwiatkowski, D. J., and Thiele, E. A. (2012) Genotype and cognitive phenotype of patients with tuberous sclerosis complex. *Eur. J. Hum. Genet.* **20,** 510–515
19. Sato, T., Nakashima, A., Guo, L., and Tamanoi, F. (2009) Specific activation of mTORC1 by Rheb G-protein *in vitro* involves enhanced recruitment of its substrate protein. *J. Biol. Chem.* **284,** 12783–12791
20. Deberardinis, R. J., Sayed, N., Ditsworth, D., and Thompson, C. B. (2008) Brick by brick: metabolism and tumor cell growth. *Curr. Opin. Genet. Dev.* **18,** 54–61
21. Coleman, P. F., Suttle, D. P., and Stark, G. R. (1977) Purification from hamster cells of the multifunctional protein that initiates *de novo* synthesis of pyrimidine nucleotides. *J. Biol. Chem.* **252,** 6379–6385
22. Iwahana, H., Fujimura, M., Ii, S., Kondo, M., Moritani, M., Takahashi, Y., Yamaoka, T., Yoshimoto, K., and Itakura, M. (1996) Molecular cloning of a human cDNA encoding a trifunctional enzyme of carbamoyl-phosphate synthetase-aspartate transcarbamoylase-dihydroorotase in *de novo* pyrimidine synthesis. *Biochem. Biophys. Res. Commun.* **219,** 249–255
23. Jones, M. E. (1980) Pyrimidine nucleotide biosynthesis in animals: genes, enzymes, and regulation of UMP biosynthesis. *Annu. Rev. Biochem.* **49,** 253–279
24. Robitaille, A. M., Christen, S., Shimobayashi, M., Cornu, M., Fava, L. L., Moes, S., Prescianotto-Baschong, C., Sauer, U., Jenoe, P., and Hall, M. N. (2013) Quantitative phosphoproteomics reveal mTORC1 activates *de novo* pyrimidine synthesis. *Science* **339,** 1320–1323
25. Ben-Sahra, I., Howell, J. J., Asara, J. M., and Manning, B. D. (2013) Stimulation of *de novo* pyrimidine synthesis by growth signaling through mTOR and S6K1. *Science* **339,** 1323–1328
26. Piao, X., Kobayashi, T., Wang, L., Shiono, M., Takagi, Y., Sun, G., Abe, M., Hagiwara, Y., Zhang, D., Okimoto, K., Kouchi, M., Matsumoto, I., and Hino, O. (2009) Regulation of folliculin (the BHD gene product) phosphorylation by Tsc2-mTOR pathway. *Biochem. Biophys. Res. Commun.* **389,** 16–21
27. Urano, J., Sato, T., Matsuo, T., Otsubo, Y., Yamamoto, M., and Tamanoi, F. (2007) Point mutations in TOR confer Rheb-independent growth in fission yeast and nutrient-independent mammalian TOR signaling in mammalian cells. *Proc. Natl. Acad. Sci. U.S.A.* **104,** 3514–3519
28. Im, E., von Lintig, F. C., Chen, J., Zhuang, S., Qui, W., Chowdhury, S., Worley, P. F., Boss, G. R., and Pilz, R. B. (2002) Rheb is in a high activation state and inhibits B-Raf kinase in mammalian cells. *Oncogene* **21,** 6356–6365
29. Liu, X., Guy, H. I., and Evans, D. R. (1994) Identification of the regulatory domain of the mammalian multifunctional protein CAD by the construction of an *Escherichia coli* hamster hybrid carbamyl-phosphate synthetase. *J. Biol. Chem.* **269,** 27747–27755
30. Carrey, E. A., Campbell, D. G., and Hardie, D. G. (1985) Phosphorylation and activation of hamster carbamyl phosphate synthetase II by cAMP-dependent protein kinase. A novel mechanism for regulation of pyrimidine

nucleotide biosynthesis. *EMBO J.* **4,** 3735–3742
31. Sancak, Y., Peterson, T. R., Shaul, Y. D., Lindquist, R. A., Thoreen, C. C., Bar-Peled, L., and Sabatini, D. M. (2008) The Rag GTPases bind raptor and mediate amino acid signaling to mTORC1. *Science* **320,** 1496–1501
32. Takahashi, K., Nakagawa, M., Young, S. G., and Yamanaka, S. (2005) Differential membrane localization of ERas and Rheb, two Ras-related proteins involved in the phosphatidylinositol 3-kinase/mTOR pathway. *J. Biol. Chem.* **280,** 32768–32774
33. Zoncu, R., Bar-Peled, L., Efeyan, A., Wang, S., Sancak, Y., and Sabatini, D. M. (2011) mTORC1 senses lysosomal amino acids through an inside-out mechanism that requires the vacuolar H^+-ATPase. *Science* **334,** 678–683